J Membrane Biol (2009) 229:141–152
DOI 10.1007/s00232-009-9180-6

Polycystic Kidney Disease Channel and Synaptotagmin Homologues Play Roles in *Schizosaccharomyces pombe* Cell Wall Synthesis/Repair and Membrane Protein Trafficking

Ebru Aydar · Christopher P. Palmer

Received: 25 March 2009 / Accepted: 2 June 2009 / Published online: 19 June 2009

Abstract Eukaryotic cells can sense a wide variety of environmental stresses, including changes in temperature, pH, osmolarity and nutrient availability. They respond to these changes through a variety of signal-transduction mechanisms, including activation of Ca^{2+}-dependent signaling pathways. This research has discovered important implications in the function(s) of polycystic kidney disease (PKD) channels and the mechanisms through which they act in the control of cell growth and cell polarity in *Schizosaccharomyces pombe* by ion channel-mediated Ca^{2+} signaling. Pkd2 was expressed maximally during the exponential growth phase. At the cell surface pkd2 was localized at the cell tip during the G_2 phase of the cell cycle, although following cell wall damage, the cell surface-expressed protein relocalized to the whole plasma membrane. Pkd2 depletion affected Golgi trafficking, resulting in a buildup of vesicles at the cell poles, and strongly affected plasma membrane protein delivery. Surface-localized pkd2 was present in the plasma membrane for a very short time and was rapidly internalized. Internalization was dependent on Ca^{2+}, enhanced by amphipaths and inhibited by gadolinium. The pkd2 protein was in a complex with a yeast synaptotagmin homologue and myosin V. Depletion of pkd2 severely affected the localization of glucan synthase. A role for pkd2 in a cell polarity and cell wall synthesis signaling complex with a synaptotagmin homologue, myosin V and glucan synthase is proposed.

E. Aydar · C. P. Palmer (✉)
Institute for Health Research and Policy, London Metropolitan University, 166-220 Holloway Road, London N7 8DB, UK
e-mail: Chris.Palmer@londonmet.ac.uk

Keywords Polycystin · pkd2 · TRP channel · Mechanosensitive · Ion channel

Introduction

In humans, autosomal dominant polycystic kidney disease (ADPKD) is one of the most commonly inherited disorders, with an incidence of approximately 1 in 1,000. The disease is characterized by the formation of large fluid-filled cysts in kidneys caused by abnormal differentiation and proliferation of kidney tubular epithelial cells, which result in chronic renal failure in 50% of patients by the age of 60. Cystic epithelial cells display changes in proliferation, apoptosis, differentiation, polarity, extracellular matrix synthesis and fluid transport. In 15% of patients, the causative mutation is located in the polycystin-2 (PKD2) gene. Evidence suggests that the polycystin complex (which includes PKD2) may act as a mechanosensor, receiving signals from the extracellular matrix, adjacent cells and tubule lumen (through cilia) and transducing them into cellular responses that regulate proliferation, adhesion, migration, differentiation and maturation, which are essential to the control of the diameter of renal tubules and kidney morphogenesis (for reviews, see Torres et al. 2007; Sutters 2006; Ong and Harris 2005; Wilson 2004). PKD2 genes are universal, being found in all organisms from yeast and fungi to vertebrates and invertebrates (Nauli et al. 2003; Palmer et al. 2005; Bok et al. 2001; Watnick et al. 2003). Our initial published work in *Schizosaccharomyces pombe* indicated that *pkd2* is an essential gene involved in a Ca^{2+} signaling pathway in a complex with a rho-GTPase. Pkd2 depletion in *S. pombe* affected cell wall synthesis, growth and cell size/shape regulation; and the protein was found to be localized to both the Golgi and plasma

membrane (Palmer et al. 2005). The *S. pombe* PKD2-related gene (designated SPAC01F7.03) was discovered by BLAST analysis and possesses significant amino acid similarity (46% in the six predicted transmembrane domains) to a PKD2-related gene called AMO (almost there) in *Drosophila melanogaster* (Palmer et al. 2005). The most similarity (59%) is observed in the fifth and sixth transmembrane domains. Transmembrane analysis plots suggested that the pkd2 gene product in *S. pombe* possesses six transmembrane domains, which are in agreement with the predictions for AMO and human PKD2 (Nauli et al. 2003; Bok et al. 2001; Watnick et al. 2003).

In mammals synaptotagmins are proposed to function as Ca^{2+} sensors and are involved in both synaptic vesicle docking and vesicle fusion to the presynaptic membrane in the regulation of neurotransmitter release and hormone secretion. Although synaptotagmins share a similar domain structure and a high degree of homology in the C2 domains, not all synaptotagmins bind to calcium (Yoon and Shin 2009). A sole gene in the *S. pombe* genome, designated SPAPYUK71.03c, was found to have 37% amino acid identity to synaptotagmin I from *Homo sapiens*. Closer examination of this predicted protein indicated that it contains four predicted C2 domains and a single predicted transmembrane domain.

Although the PKD complex in humans has been implicated in mechanosensation (Nauli et al. 2003), it is still not clear which part of this complex actually is the mechanosensing unit. At present, some researchers favor PKD1 (Forman et al. 2005) since the PKD2 channel has been reported to be a nonselective cation channel (Hanaoka et al. 2000). Two not necessarily mutually exclusive hypotheses state that polycystin-2 is located in the endoplasmic reticulum, Golgi membrane and/or plasma membrane (Tsiokas et al. 2007). Finally, the molecular mechanisms governing the control of cell growth and polarity have advanced due to the study of this process in *S. pombe* and *Saccharomyces cerevisiae* (Humphrey and Pearce 2005; Sveiczer et al. 2004; Sawin 2002). The aim of this work was thus to answer some basic questions concerning PKD2-related genes, using *S. pombe* as a model organism, and to determine the role of Pkd2 in *S. pombe* in the control of cell wall synthesis/repair, growth, polarity and membrane trafficking.

Experimental Procedures

Materials

PBS contained 1.9 mM NaH_2PO_4, 8.1 mM Na_2HPO_4, 150 mM NaCl (final pH 7.4); PEM contained 100 mM PIPES (pH 6.9), 1 mM EGTA, 1 mM $MgSO_4$; PEMS PEM contained 1 M sorbitol; PEMB PEM contained 1% BSA; cell lysis involved Tris-HCl (pH 7.4), 1 mM EDTA, 1% Triton X-100, 150 mM NaCl, 1 mM dithiothreitol; TBST Tris-HCl (pH 8.0) contained 125 mM NaCl, 0.1% Tween 20. Rabbit anti-hemagglutinin (HA; Invitrogen, Paisley, UK), mouse anti-green fluorescent protein (GFP, Invitrogen), mouse anti-C-myc (Invitrogen), anti-mouse FITC (Dako, Cambridge, UK), anti-rabbit FITC (Dako), anti-mouse Alexa Fluor 568 (Invitrogen), anti-rabbit Alexa Fluor 568 (Invitrogen), anti-mouse horseradish peroxidase (HRP, Dako), anti-rabbit HRP (Dako) and rabbit anti-pkd2 were also used (see "Generation and Characterization of an Antibody to the *S. pombe* pkd2 Protein").

Generation and Characterization of an Antibody to the *S. pombe* pkd2 Protein

A polyclonal antibody to a peptide localized just after the predicted fifth transmembrane domain (Palmer et al. 2005) of the *S. pombe* pkd2 protein (PYATKHMNTLHIH) was generated in rabbits. The titer of the rabbit serum 74 days after injection was characterized by ELISA against the peptide. Specific antibodies were purified from the rabbit sera using immobilized peptide and again titrated by ELISA. The concentration of the purified antibody was 35 μg/ml. Cell lysates (5 μg/lane) prepared from *S. pombe* were separated on SDS-PAGE gels and Western-blotted. The blots were probed with the purified antibody (1 μg/ml) and subsequent detection as described in "Immunofluorescence, Golgi Labeling and Confocal Microscopy". A single band at 75 kDa was observed. This band was not observed when the antibody was preabsorbed with the peptide used to generate the antibody.

S. pombe Methodology and Materials

All general methods for *S. pombe* culture and genetic manipulation were as described previously (Moreno et al. 1991). Strains were grown in Edinburgh minimal medium (EMM) with appropriate supplements unless stated otherwise (Moreno et al. 1991). pREP41x and pREP42x are leucine or uracil *S. pombe* vectors containing low-strength, thiamine-repressible promoters, as described previously (Craven et al. 1998). Pkd2 depletion was achieved using the strain 96116 Δ*pkd2*::*his3* with thiamine-repressible promoter expression plasmid pREP41x-*pkd2*. Generally, depletion was achieved by incubation in EMM containing thiamine (Craven et al. 1998) for 16 or 24 h, as specified in the figure legends. Strain 96116, h + his3-D1 leu1-32 ura4-D18 ade6-M210, was obtained from the ATCC (Manassas, VA). All other strains were derived from this. The *pkd2* knockout strain 96116 Δ*pkd2*::*his3* is as previously described (Palmer et al. 2005). For a list of strains with transformed plasmids used, see Table 1.

Table 1 *S. pombe* strains containing expression plasmids utilized in this investigation

S. pombe strain
96116 Δ*pkd2*::*his3* pREP41x-*pkd2* (as described by Palmer et al. 2005)
96116 Δ*pkd2*::*his3* pREP42x-*pkd2-myc* & pAL-*gms1*-GFP & pFS119-*aap1*-HA
96116 Δ*pkd2*::*his3* pREP41x-*pkd2-myc* & pREP42x-HA-*syn1*
96116 Δ*pkd2*::*his3* pREP41x-*pkd2-myc* & pREP42x-*syn1*-HA
96116 Δ*pkd2*::*his3* pREP42x-*pkd2-myc* & pREP41x-*myo5.1*-HA
96116 Δ*pkd2*::*his3* pREP42x-*pkd2-myc* & pREP41x-*myo5.2*-HA
96116 Δ*pkd2*::*his3* pREP42x-*pkd2-myc* & pREP41-GFP-*myo5.2*
96116 Δ*pkd2*::*his3* pREP42x-*pkd2-myc* & *pJK*-GFP-*bgs1*

Immunofluorescence, Golgi Labeling and Confocal Microscopy

For immunostaining of unpermeabilized cells, *S. pombe* cultures were grown to an OD_{600} of 0.5–0.8. The cells were collected by centrifugation and resuspended in cold PBS. Primary antibody was added, diluted in PBS with 1% BSA at a concentration of 10 μg/ml and incubated with rotation for 2 h at 4°C. The cells were washed by centrifugation and resuspension with PBS four times, anti-mouse or anti-rabbit FITC or Alexa Fluor 568-congugated secondary antibodies (at the manufacturers' suggested concentrations) were added and the mixture was diluted in PBS with 1% BSA and incubated with rotation for 2 h at 4°C in the dark. The cells were again washed four times with PBS and finally resuspended in a small volume of PBS. Cells were mounted by drying a smear of cells on a glass slide and mounted with coverslips using VectorShield mounting media (VectorLabs, Peterborough, UK). For immunofluorescence of permeabilized cells, cultures were grown to an OD_{600} of 0.5–0.8 and fixed in 4% formaldehyde in PEM buffer at 30°C for 1 h. Cells were collected by centrifugation and washed four times by centrifugation in PEM buffer. The cell wall was digested by resuspending the cells at a density of 5×10^7/ml in PEMS buffer containing 1 mg/ml of Novozym 234 (Novo, Bagswaerd, Denmark) and 0.3 mg/ml of zymolyase 20T for 20 min at 37°C. Cells were recollected by centrifugation and washed three times with PEMS buffer. Cells were permeabilized by resuspension in 1% Triton X-100 in PEMS buffer for 2 min at room temperature. Following a further two washes in PEM, the cells were incubated for 30 min in PEM with 5% BSA at room temperature. After a further wash in PEM primary and secondary antibodies were added as in the above protocol except that PEM buffer was used instead of PBS. Cells were mounted as described below. Golgi labeling was performed using 4,4-difluoro-4-bora-3a,4a-diaza-s-indacene (BODIPY) TR C5-ceramide (Molecular Probes, Eugene, OR). BODIPY TR C5-ceramide (5 mg) was dissolved in 10 mM HEPES (pH 7.4) to a stock concentration of 0.5 mM. Mid-exponential phase cells were spun and washed in ice-cold 10 mM HEPES (pH 7.4), and BODIPY TR C5-ceramide was added at a working concentration of 50 μM. The cells were incubated at 4°C for 30 min and subsequently washed four times in ice-cold 10 mM HEPES (pH 7.4). The cells were finally resuspended in YES medium and incubated at 30°C for 30 min with agitation before mounting for confocal microscopy using VectorShield mounting media. Confocal microscopy was performed on a Leica (Nussloch, Germany) 650T instrument using 568 nm and 488 nm filters. Colocalization was performed using Image J (National Institutes of Health, Bethesda, MD).

Cell Lysis and Fractionization

Cell lysis was performed by collection using centrifugation ($300 \times g$ for 20 min at 4°C) and resuspension of cells at an OD_{600} of 50 in cell lysis buffer containing proteinase inhibitors (Roche, Welwyn Garden City, UK). An equal volume of glass beads (0.4 μM diameter) was added to the suspension. The cells were lysed using a cycle of vortexing (30 s vortex/30 s on ice) for 15 min. Subsequently, the cells were incubated on ice for 30 min and then centrifuged at $5{,}000 \times g$ for 20 min at 4°C. The supernatant was removed and stored at –80°C. Cell lysates prepared as described above were standardized by adjusting to 1 mg/ml of protein with lysis buffer (as above). The lysate (1 ml) was loaded at the top of a 20–53% continuous sucrose gradient in 13-ml SW41 centrifuge tubes and spun at $100{,}000 \times g$ for 15–16 h for membranes to reach equilibrium density. Ten 1.2-ml fractions were removed from the bottom of the tube by puncturing the tube with a needle.

Surface Biotin Labeling of Cells and Streptavidin Purification of Biotinylated Proteins

S. pombe cells were grown to an OD_{600} of 0.5–0.8 in EMM with appropriate supplements. After three washing steps by centrifugation in cold PBS (pH 7.4), cells were incubated for 2 h at 4°C with 10 mg/ml sulfo-*N*-hydroxysuccinimido (NHS)-LC-biotin (membrane-impermeable reagent, Molecular Probes) in binding buffer 50 mM $NaHCO_3$ (pH 8.5) at an OD_{600} of 50. The remaining reactive sulfo-NHS-LC-biotin was blocked by adding 2 vol of 100 mM Tris-HCl (pH 8.0) and further incubation for 1 h at 4°C. Aliquots of cells were harvested by centrifugation at $300 \times g$ for 20 min at 4°C, washed once in cold PBS (pH 7.4) and twice in cold EMM and resuspended in cold EMM at an OD_{600} of 0.5. Biotinylated proteins were purified from cell lysates using Immunopure-immobilized avidin and a classic Seize immunoprecipitation kit (Pierce, Rockford, IL).

Slot and Western Blotting

Protein samples in a volume of 100 µl were applied to nitrocellulose membranes using a slot blotting apparatus. The blots were blocked with a solution containing 2.5% skimmed milk and 2.5% BSA in TBST overnight at 4°C prior to probing with epitope- or pkd2-specific antibodies. Protein samples at a concentration of 1 mg/ml were mixed with SDS sample buffer (Sigma, Dorset, UK), and 5 µg of protein were loaded per lane and separated on acrylamide 4–20% gradient Tris-glycine minigels (Cambrex, East Rutherford, NJ). The proteins were transferred to nitrocellulose membranes for 2 h at 4°C, and the blots were blocked with a solution containing 2.5% skimmed milk and 2.5% BSA in TBST overnight at 4°C prior to probing with pkd2- or epitope-specific antibodies. Even blot transfer was verified using Ponceau red staining. Immunoblots were probed with antibodies to various epitopes (HA, c-myc, GFP) or pkd2. The antibodies were diluted to 1 µg/ml in TBST with 0.5% skimmed milk and 0.5% BSA and incubated with the blot for 2 h at room temperature. Following four 10-min washes with TBST (with constant agitation) at room temperature, the blots were incubated with anti-mouse or anti-rabbit HRP-congugated secondary antibodies (at the manufacturers' suggested concentrations) as appropriate and diluted in TBST with 0.5% skimmed milk and 0.5% BSA for 2 h at room temperature. The blots were again washed as before and then developed with either an ECL Advance Western blot kit or an ECL kit (GE HealthCare Limited, UK). Slot blots were quantified using Image J (National Institutes of Health) and expressed as a percentage of the total optical density of each slot blot.

Immunoprecipitation

Cell lysates were prepared as described above and adjusted to a protein concentration of 1 mg/ml, and an epitope-specific antibody was added (10 µg to 1 ml of lysate) and incubated at room temperature for 4 h on a rotating wheel. Immunoprecipitation was performed using a Classic A Immunoprecipitation kit (Pierce), according to the manufacturer's instructions. Following elution, the samples were mixed with 2 × SDS sample buffer (Sigma). Samples were separated by SDS-PAGE and Western blotting to nitrocellulose, followed by immunoblotting with epitope-specific antibodies, subsequent detection with an anti-mouse or anti-rabbit HRP-congugated secondary antibody as appropriate and development with an ECL Advance Western blot kit (GE HealthCare Limited).

Means and standard errors were calculated from the data, and the significance of results was analyzed using a one-way ANOVA at a 95% confidence level.

Results

Surface Localization of pkd2 Protein During the Cell Cycle

Previous studies suggested that the pkd2 protein was expressed as a minor fraction at the cell surface (by surface biotinylation experiments [Palmer et al. 2005]). To further investigate pkd2 surface localization, we generated an antibody to a region of the channel just after the predicted fifth transmembrane domain. Cell lysates (5 µg/lane) prepared from *S. pombe* were separated on SDS-PAGE gels and Western-blotted. The blots were probed with the purified antibody (1 µg/ml) and subsequent detection as described in "Experimental Procedures." A single band at 75 kDa was observed (Fig. 1a). This band was not observed when the antibody was preabsorbed with the generating peptide ($n = 5$). Immunofluorescent studies on unpermeabilized cells using this antibody revealed expression of pkd2 at the cell surface but only at the tip of the cell. Normally, only 5 ± 1% of cells were stained ($n = 5$). Most of the stained cells (98 ± 2%) possessed single punctate expression at the tip of the cell (Fig. 1b). The remainder of the stained cells (2 ± 1%) possessed more extensive staining at the cell tip (Fig. 1b). Very occasionally (>0.1%), both ends of the cell were stained (not shown). These results also indicate that the region just after the fifth transmembrane domain of pkd2 is accessible at the extracellular side of the cell. Further controls are shown in Fig. 1c. To characterize pkd2 surface localization during the cell cycle, a *cdc25-22* strain was synchronized by arresting at the G_2/M boundary (Booher et al. 1989). Following temperature release, the unpermeabilized cells were stained with the pkd2 antibody and the number of cells stained was plotted against the septation index (Fig. 1d). At 4 h postrelease, septation was found to be at its peak (68 ± 4%). Following this time point, pkd2 labeling increased from 0% to 36%, while septation decreased to 10 ± 1% at 6 h postrelease. This increase in pkd2 labeling was stastistically significant ($P = 3.2 \times 10^{-3}$, $F = 68$, $n = 6$). The results indicated that pkd2 is expressed at the cell surface during the G_2 phase and expression is minimal during septation ($n = 5$).

pkd2 Is Expressed Maximally During the Exponential Growth Phase and its Localization Changes following Damage to the Cell Wall

Expression of total pkd2 (whole-cell lysate protein) and surface pkd2 (surface-biotinylated protein) during cell growth was monitored by protein extraction from cells, slot blotting to nitrocellulose followed by detection with an antibody to pkd2. The greatest pkd2 expression (total and surface) was observed during the exponential phase of cell

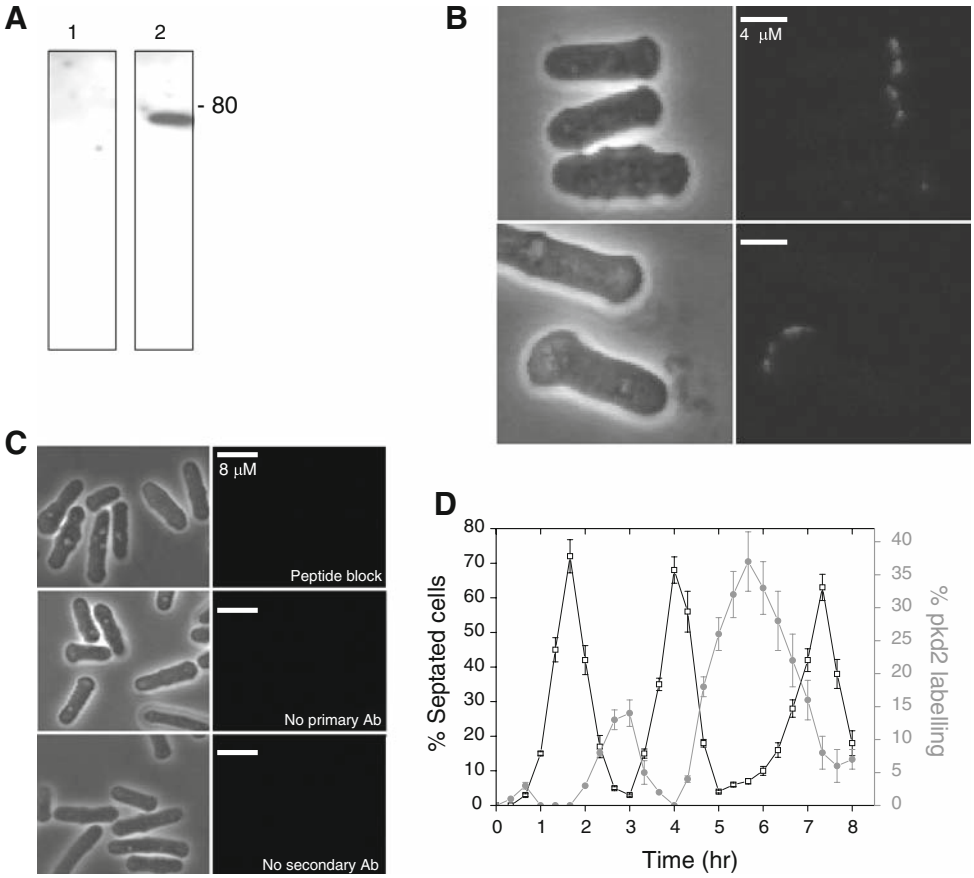

Fig. 1 Surface localization of pkd2 protein during the cell cycle. **a** Immunoplot staining of *S. pombe* cell extracts with an antibody generated to pkd2. *Lane 1*, The antibody was incubated with the peptide against which it was generated. Size of marker proteins (in kDa) is indicated to the side of all blots. **b** Confocal microscopy of immunolabeled *S. pombe* cells (unpermeabilized) with an antibody derived against 20 amino acids just after the predicted fifth transmembrane domain. *Left panel*, phase contrast; *right panel*, immunofluorescence. **c** Examples of controls, including peptide block of the antibody before immunostaining, no primary antibody and no secondary antibody. *Left panel*, phase contrast; *right panel*, immunofluorescence. **d** Proportion of pkd2 immunostained cells plotted against septation index in unpermeabilized *cdc25-22* cells following release from synchronization

growth and sharply cut off once stationary phase was reached (Fig. 2a). Following damage of the cell wall with zymolyase (0.2 μg zymolyase-100T/ml for 20 min), total pkd2 protein expression was found to significantly increase by almost double ($P = 3.2 \times 10^{-6}$, $F = 124$, $n = 6$), while surface expression increased significantly by over 10-fold 20 min after cell wall damage ($P = 3.9 \times 10^{-6}$, $F = 321$, $n = 6$) (Fig. 2b). It may be reasoned that zymolyase treatment causes an increase in the exposure of the antibody to pkd2, thus increasing antibody staining. However, in stationary cells no significant increase in the small amount of pkd2 staining was observed following zymolyase treatment (data not shown). Confocal microscopy of unpermeabilized cells stained with a pkd2 antibody following cell wall damage indicated an increase in pkd2 surface expression (Fig. 2c).

Golgi Trafficking/Plasma Membrane Protein Delivery Defect in pkd2-Depleted cells

Phase-contrast microscopy of pkd2-depleted cells revealed the presence of numerous vesicles within the cell generally localized toward the poles (Fig. 3a). To investigate whether this may be due to a buildup of Golgi vesicles, we stained pkd2-depleted cells with the Golgi dye BODIPY TR C5-ceramide. In pkd2-depleted cells we observed a concentration of Golgi-specific staining, particularly at the cell poles (Fig. 3b). Since ADPKD patients have been found to possess aberrant Golgi function and basolateral exocytosis in renal epithelia (Charron et al. 2000), we investigated the effect of pkd2 depletion on the delivery of membrane proteins to the plasma membrane using an epitope-tagged amino acid permease (aap1), which is normally localized to the plasma membrane (Ding et al. 2000). By subcellular fractionation of cells expressing aap1-HA and gms1-GFP (a Golgi-resident protein [Tanaka and Takegawa 2001]) fusion proteins, we observed that upon pkd2 depletion the aap1 protein was no longer found predominantly in the plasma membrane but mislocalized in the Golgi fraction (Fig. 3c). In plasma membrane fraction 2 aap1-HA decreased from 32 ± 4% to 8 ± 2% upon pkd2 depletion, while in Golgi fraction 7 aap1-HA increased from 2 ± 1% to 29 ± 5% upon pkd2 depletion. Both of these changes were statistically significant ($P = 1.2 \times 10^{-6}$, $F = 137$, $n = 4$; $P = 1.7 \times 10^{-7}$, $F = 156$, $n = 4$).

Amphipaths and Gadolinium Affect the Growth of pkd2-Depleted Cells

Since pkd2 channels have been implicated in mechanosensation (Nauli et al. 2003) and our hypothesis is that

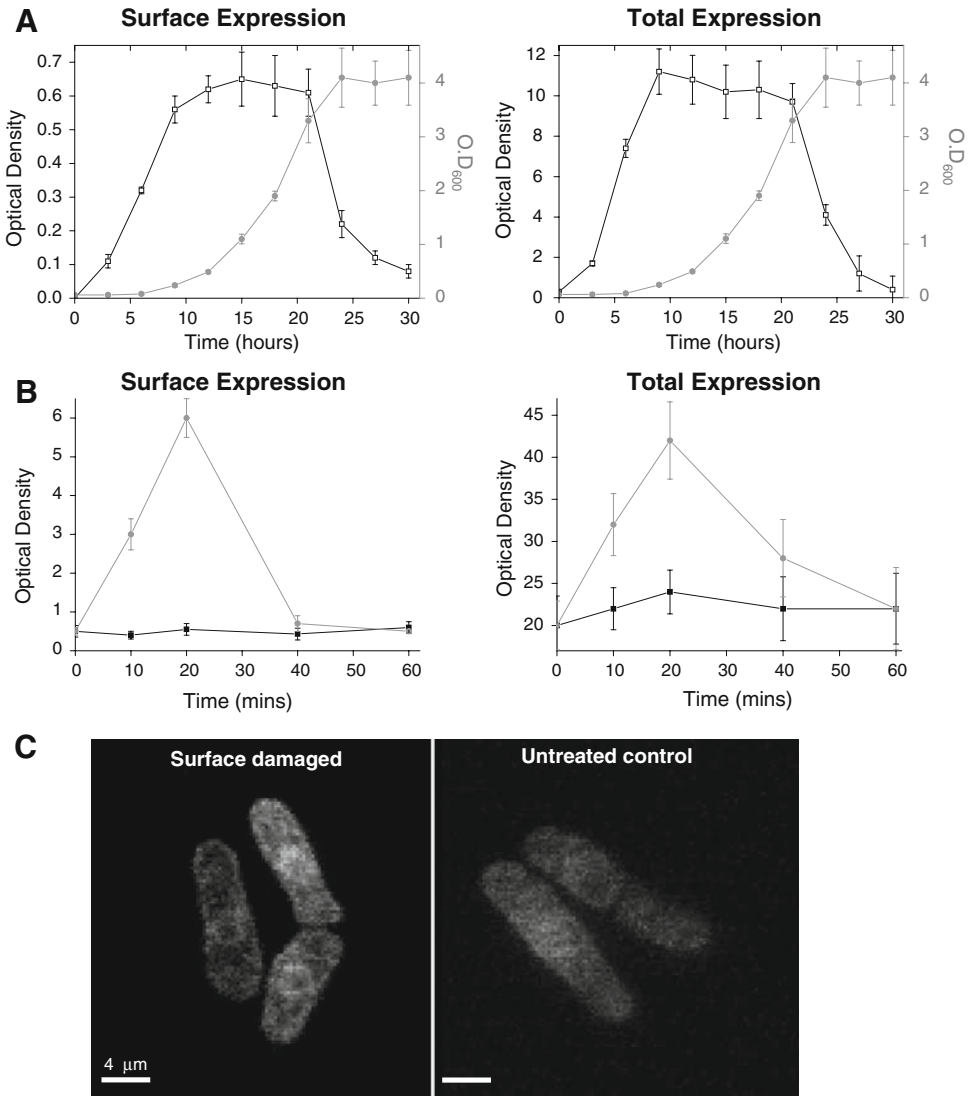

Fig. 2 pkd2 is expressed maximally during the exponential growth phase, and its localization changes following damage to the cell wall. **a** Surface and total expression of pkd2 protein monitored by immunoblotting of whole-cell lysates and immunocaptured surface biotinylated protein. Stationary-phase cells were inoculated at an OD of 0.05, and samples were taken every 3 h. **b** Surface and total expression of pkd2 protein monitored by immunoblotting of whole-cell lysates and immunocaptured surface biotinylated protein following cell wall damage using zymolyase (*circles*) or mock treatment (*squares*). **c** Confocal microscopy of *S. pombe* pkd2-GFP expressing strain following cell wall damage with zymolyase

pkd2 may encode a mechanosensitive ion channel, we tested the affect of amphipaths and gadolinium (modulators of mechanosensitive ion channels [Qi et al. 2005]) on the growth of the pkd2-depleted strain. Cells were depleted of pkd2 for 24 h, and the cell density was adjusted to an OD_{600} of 0.5. The cultures were treated with nothing (control), 10 µm lysophosphatidylcholine (LPS-choline), 10 µm lysophosphatidylinositol (LPS-inositol) or 10 µm gadolinium for 4 h at 30°C. Subsequently, cell growth was quantified by measuring the OD_{600} values (Fig. 4). Growth of the wild-type strain was not affected by these treatments (data not shown). For the pkd2-depleted strain LPS-choline significantly increased cell growth ($P = 1.7 \times 10^{-4}$, $F = 122$, $n = 5$). LPS-inositol, a more severe amphipath, significantly increased cell growth compared to LPS-choline ($P = 2.2 \times 10^{-4}$, $F = 178$, $n = 5$). Gadolinium reduced the growth rate of the pkd2-depleted strain compared to the untreated cells, and this difference was significant ($P = 1.1 \times 10^{-4}$, $F = 89$, $n = 5$).

Rapid Internalization of Plasma Membrane–Localized pkd2

The punctate surface staining of pkd2 in *S. pombe* suggested to us that the localization of pkd2 in the plasma membrane may be transient. *S. pombe* cells were surface-biotinylated in order to label the pkd2 protein present at the cell surface. Subsequently, the cells were incubated at 30°C for different times (1, 4 and 10 min), and the fate of the surface-labeled pkd2 was monitored by sucrose density gradient centrifugation (to separate different cell fractions). To access the localization of Golgi and plasma membrane fractions, we utilized a strain expressing an aap1-HA fusion (plasma membrane amino acid permease [Ding et al. 2000]) and a gms1-GFP fusion (a Golgi-resident protein [Tanaka and Takegawa 2001]). Following centrifugation ten fractions were collected and either fractions were directly slot-blotted to nitrocellulose (in the case of aap-HA and gms1-GFP detection) and probed with epitope-specific

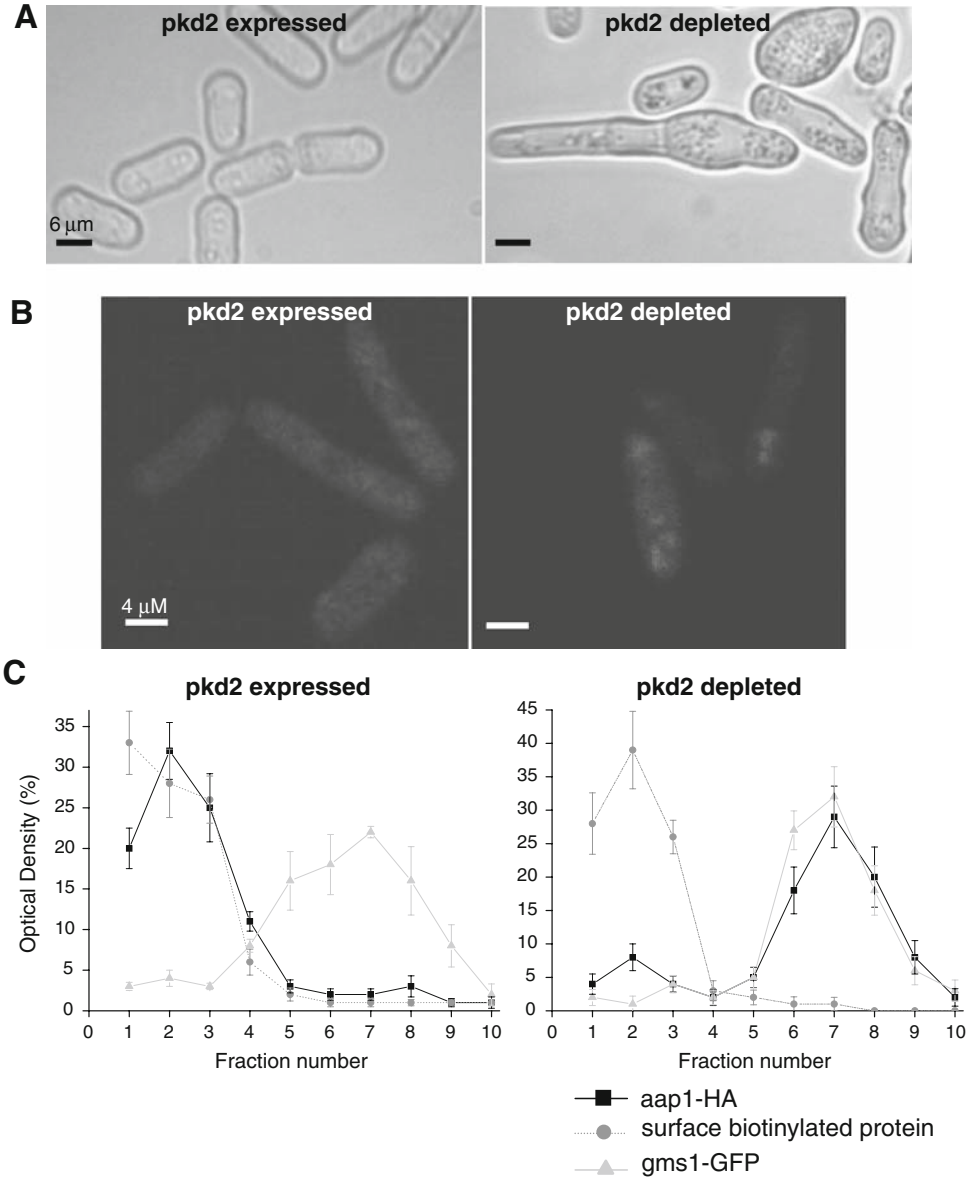

Fig. 3 pkd2-depleted cells are defective in plasma membrane protein transport and have an abnormal Golgi. **a** Cells were depleted of pkd2 for 16 h and visualized by phase-contrast microsopy. Numerous vesicle-like structures can be seen accumulating at the poles of the cells. **b** Confocal microsopy of pkd2-depleted cells stained with BODIPY TR C5-ceramide to visualize Golgi staining. **c** Localization of the plasma membrane protein aap1 in pkd2-depleted cells

antibodies or the biotinylated protein was immunopurified and the eluted protein was slot-blotted to nitrocellulose and detected using a pkd2-specific antibody. The quantified results (Fig. 5a) indicated that surface pkd2 protein is rapidly internalized (within 10 min) following incubation at 30°C. Biotinylated pkd2 in fraction 2 (plasma membrane fraction) changed from 47 ± 5% to 3 ± 1% following incubation at 30°C, which was statistically significant ($P = 1.6 \times 10^{-4}$, $F = 117$, $n = 4$), while in fraction 6 (Golgi fraction) it changed from 0 to 35 ± 5% ($P = 2.2 \times 10^{-11}$, $F = 421$, $n = 4$). In cells held at 4°C no internalization occurred. As a comparison, the plasma membrane protein aap1 was also monitored by surface biotinylation, and we found no internalization of this protein after 10 min at 30°C.

Amphipaths and Gadolinium Affect the Internalization of Plasma Membrane–Localized pkd2

Since the growth of pkd2-depleted cells was affected by amphipaths and gadolinium and given the rapid pkd2 internalization observed, we decided to investigate factors which may affect this internalization. Pkd2 is a transient receptor potential (TRP)–like channel, and pkd2 depletion results in a Ca^{2+}-sensitive phenotype (Palmer et al. 2005); thus, we investigated the effect of Ca^{2+} removal on pkd2 internalization. We found that removal of Ca^{2+} (using EMM without Ca^{2+} and with 1 mM EGTA) inhibited the internalization of pkd2 (Fig. 5b). Biotinylated pkd2 in fraction 6 (Golgi fraction) was not significantly altered, from 0 ± 0% to 0.5 ± 0.1%, upon incubation at 30°C with EGTA

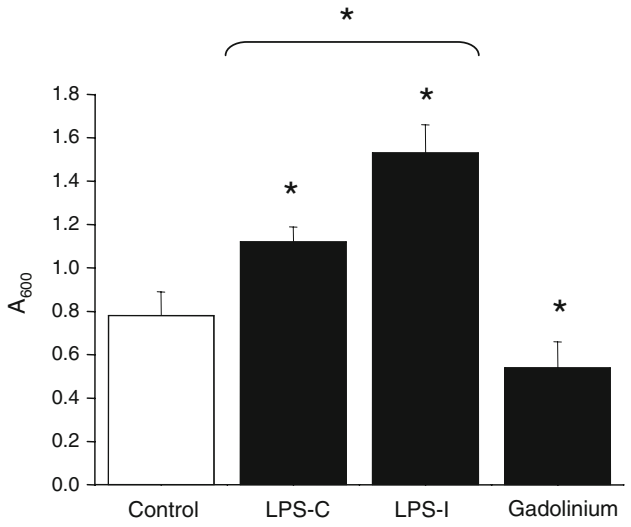

Fig. 4 Mechanosensitive ion channel modulators affect the growth of pkd2-depleted cells. Cells were depleted of pkd2 for 24 h, and cell density was adjusted to an OD_{600} of 0.5. Cultures were treated with nothing (control), 10 μm LPS-choline, 10 μm LPS-inositol or 10 μm gadolinium for 4 h at 30°C. Subsequently, cell growth was quantified by measuring OD_{600} values. Growth of the wild-type strain was not affected by these treatments (data not shown). *Significant at 95% confidence level

($P = 0.35$, $F = 0.9$, $n = 4$). This was different when the cells were incubated at 30°C without EGTA, where fraction 6 increased significantly to $15 \pm 4\%$ ($P = 1.4 \times 10^{-2}$, $F = 59$, $n = 4$). The PKD complex has been implicated in mechanosensation (Nauli et al. 2003). The amphipath LPS-choline (LPS-choline forms cup-like crenellations in the plasma membrane and, as such, is known to activate mechanosensitive ion channels [Qi et al. 2005]) was found to significantly increase the rate of pkd2 internalization. In fraction 6 biotinylated pkd2 increased from $15 \pm 4\%$ to $47 \pm 7\%$ ($P = 4.5 \times 10^{-3}$, $F = 89$, $n = 4$) (Fig. 5b), while gadolinium (which acts by inhibiting the fluidity of the plasma membrane [Petrov and Martinac 2007] and is known to be an inhibitor of mechanosensitive ion channels) was found to completely block pkd2 internalization. In fraction 6 no biotinylated pkd2 ($0 \pm 0\%$) was found when the cells were treated with gadolinium, which was significantly different in the absence of gadolinium, $15 \pm 4\%$ ($P = 1.2 \times 10^{-9}$, $F = 323$, $n = 4$).

Pkd2 Interacts and Colocalizes with a Synaptotagmin-Like Molecule

Our data suggested that pkd2 is involved in a Ca^{2+} signaling pathway, which involves membrane trafficking. As such, we searched the *S. pombe* genome for a likely Ca^{2+} sensor in this signaling pathway. We found that a synaptotagmin-like protein (predicted product of the SPAPYUK71.03c gene, referred to as syn1) was in an immunoprecipitable complex with pkd2 protein (Fig. 6a). The intracellular and surface localization of synaptotagmin was investigated. The intracellular localization of syn1 was found to be identical to that of pkd2 (Fig. 6b) as punctate vesicles within the cytoplasm colocalizing with Golgi staining (Palmer et al. 2005). The syn1 protein was expressed with an HA tag at either its N or its C terminus. In cells with an N terminus–tagged syn1 we found labeling in unpermeabilized cells at the tip of the cell, while no labeling was seen in the C terminus–tagged syn1, although labeling was observed in permeabilized cells (data not shown). Co-immunostaining of pkd2 and N terminus–tagged syn1 in unpermeabilized cells indicated colocalization. Indeed, syn1 staining was only observed in cells which also possessed pkd2 staining.

Pkd2 Interacts and Partially Colocalizes with Myosin V and Glucan Synthase

Myosin V activity has been found to be necessary to efficiently localize the beta-1,3-glucan synthase bgs1, either at the cell poles or at the division septum, regions of cell wall deposition (Cortes et al. 2002). We found that myo5.2, but not myo5.1, was in an immunoprecipitable complex with pkd2 protein ($n = 3$) (Fig. 7a). Additionally, where pkd2 was expressed myo5.2 was also found to colocalize (Fig. 7b). Glucan synthase (bgs1) was not found to be in an immunoprecipitable complex with pkd2 (data not shown), although rho1 (which is bound to glucan synthase) was (Palmer et al. 2005; Arellano et al. 1996). However, surface-localized pkd2 was found to colocalize with bgs1 (Fig. 7c). Upon pkd2 depletion, bgs1 localization was severely altered (Fig. 7d). In control cells bgs1 was localized to the cell tips and septum. Upon pkd2 depletion, bgs1 localization was no longer found only at the cell tips but also along the length of the cell or, as in most cases, at sporadic spots at the cell surface; many cells did not possess any bgs1 staining. Pkd2 depletion reduced the total number of cells which contained septae (data not shown). In the few cells that contained septae bgs1 localization was found to be normal (Fig. 7d).

Discussion

ADPKD patients have been found to possess aberrant Golgi function and basolateral exocytosis in renal epithelia (Charron et al. 2000). Similarly, in S. *pombe* aberrant Golgi staining was observed following pkd2 depletion. The trafficking of plasma membrane proteins was severely disrupted as indicated by a buildup of amino acid permease at the cell pole. The intracellular location of polycystin-2 is a debated topic in the field of PKD (Tsiokas et al. 2007). In

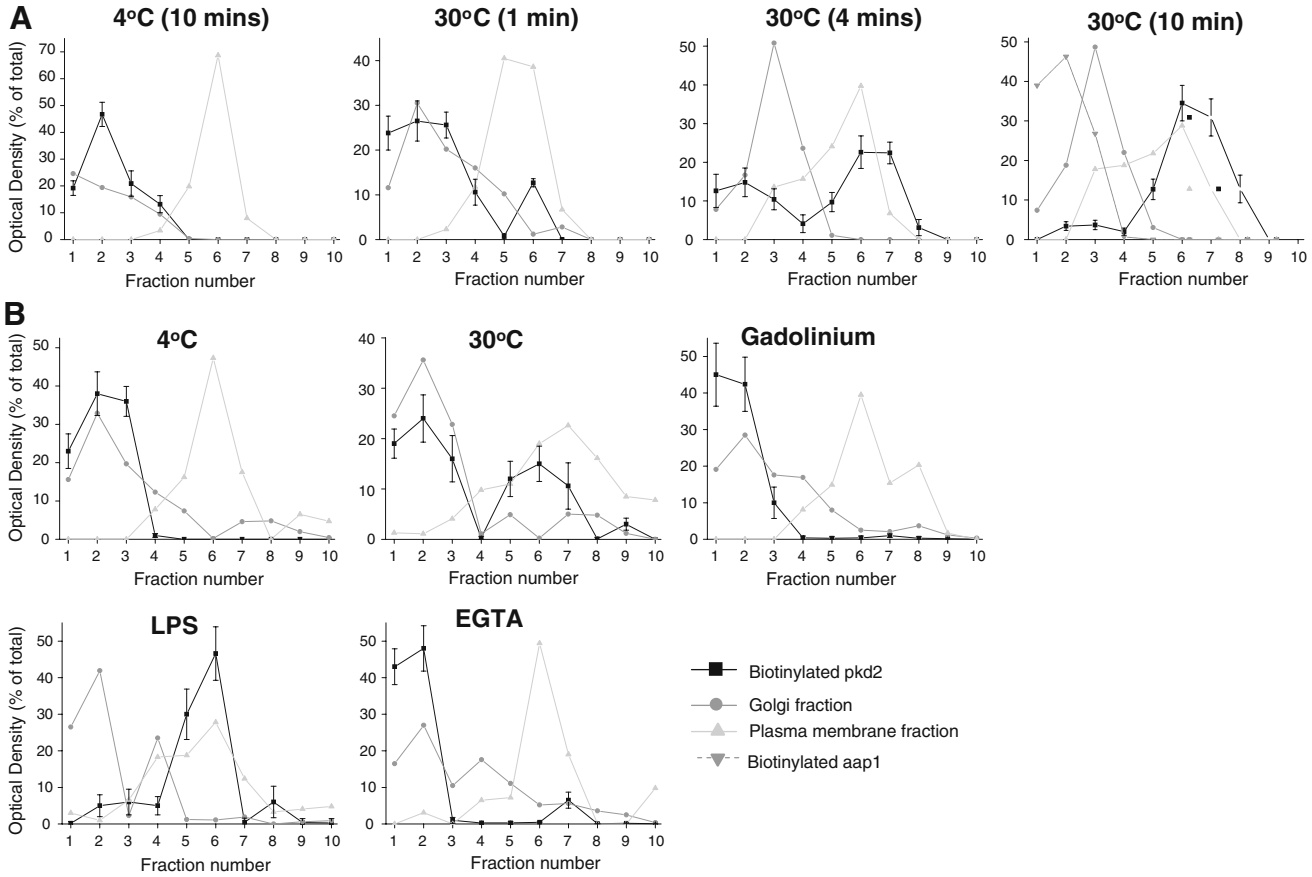

Fig. 5 Rapid internalization of plasma membrane–localized pkd2 and effect of amphipaths and gadolinium on this process. Subcellular localization of surface biotinylated pkd2 following incubation at 30°C for different times. **a** Surface biotinylated labeled cells (expressing aap1-HA and gms1-GFP fusions) were incubated at 30°C for different times (1, 4 and 10 min) and subsequently lysed, and subcellular fractions were separated by sucrose gradient centrifugation. **b** Surface biotinylated labeled cells (expressing aap1-HA and gms1-GFP fusions) were incubated at 30°C for 10 min in the presence of gadolinium, using EMM without Ca^{2+} and with 1 mM EDTA or LPS. Fractions were split and either fractions were slot-blotted directly to nitrocellulose or biotinylated protein was immunocaptured and then slot-blotted. Blots were probed with antibodies to pkd2, HA to detect aap1 (plasma membrane fraction) or GFP to detect gms1 (Golgi fraction). As controls the cells were also incubated at 4°C for 10 min. For comparison, blots were also probed for surface biotinylated aap1. Immunoblots from the above experiment were quantified, and the OD of each slot was expressed as a percentage of the total OD in each blot plotted against the fraction number (1–10) for each treatment

S. pombe the pkd2 protein can be found in Golgi and plasma membrane fractions. In normal cells pkd2 was found as punctate vesicles within the cell cytoplasm colocalizing with the Golgi membrane (as previously reported [Palmer et al. 2005]). This expression was maximal during exponential growth. Following cell wall damage, pkd2 expression increased and its localization changed to predominantly plasma membrane and endoplasmic reticulum, with the surface localization increasing by sixfold. Pkd2 is found at the cell surface but localized only at the tip of growing cells (in normal cells). Expression at the cell poles is maximal during the G_2 phase of cell growth.

The punctate pattern of pkd2 staining found at the cell tip suggested that pkd2 localization in the plasma cell membrane may be transient. Our experiments indicated that surface-localized pkd2 is rapidly internalized within 10 min compared to other plasma membrane proteins. This process was found to be Ca^{2+}-dependent; it is feasible that Ca^{2+} entry following pkd2 activation may result in its own internalization, thus removing the channel from the plasma membrane once its function is complete.

We speculated that pkd2 may encode a mechanosensitive ion channel. Amphipaths such as LPS-choline were found to increase the proliferation of pkd2-depleted cells, and the more potent amphipath LPS-inositol had a more significant effect, while gadolinium had the opposite effect, decreasing cell proliferation. Similarly, our results indicated that amphipaths and gadolinium affected the internalization of plasma membrane–localized pkd2. Amphipaths such as LPS-inositol are known to be "cup formers" in that they create cup-like crenellations in the cell membrane (Qi et al. 2005). As such, they are known to be activators of

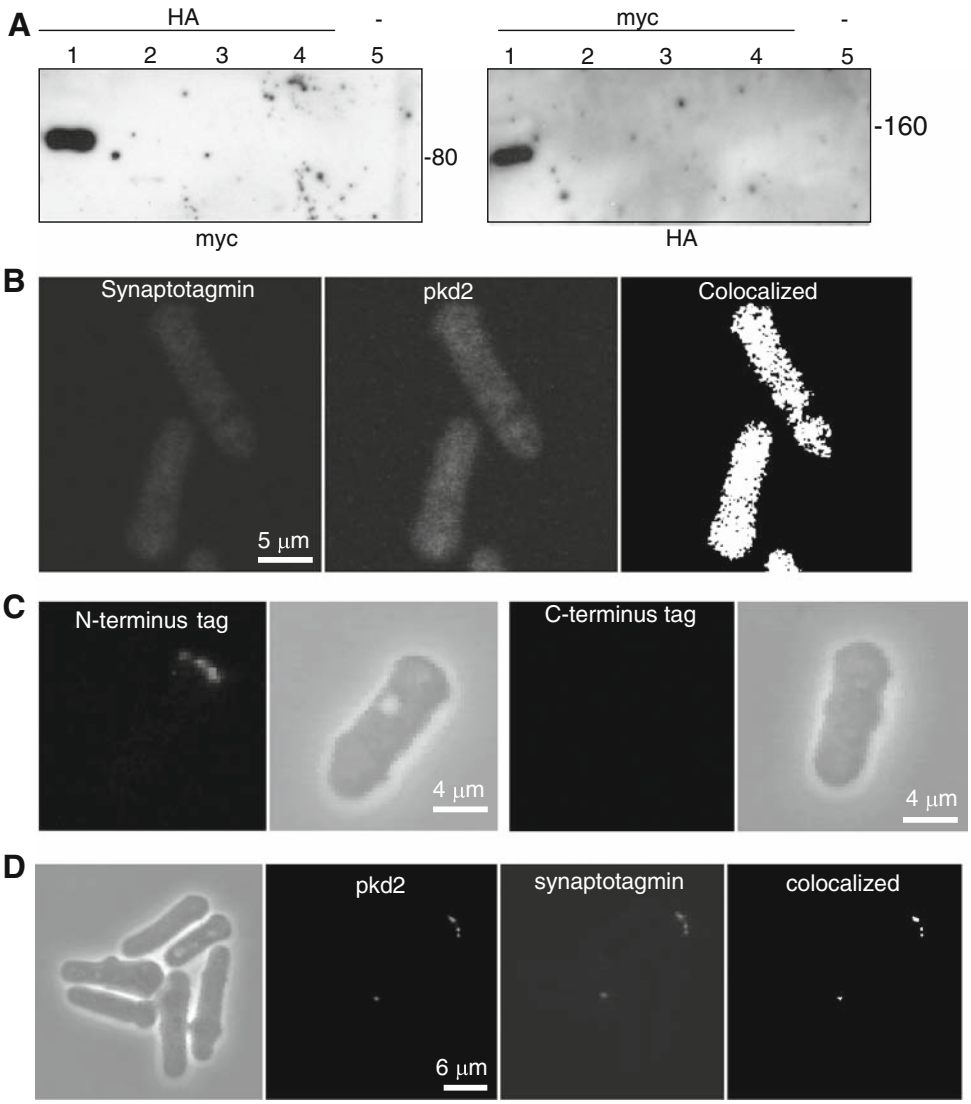

Fig. 6 Pkd2 interacts and colocalizes with a synaptotagmin-like molecule. **a** Western blots depicting pkd2 interaction with syn1. Cell lysates were prepared from cells expressing the following tagged constructs and used for immunoprecipitation. The immunoprecipitates were loaded and separated on SDS 10% PAGE and then analyzed by immunoblotting. *Lanes 1* and *5*, pkd2-myc and syn1-HA; *lane 2*, pkd2-myc; *lane 3*, syn1-HA; *lane 4*, null. The immunoprecipitating antibody is shown above each blot, and the antibody used as a Western blot probe is indicated below each blot. Size of marker proteins (in kDa) is indicated to the side of all blots. **b** Co-immunostaining of permeabilized cells expressing pkd2-myc and syn1-HA constructs. **c** Immunostaining of unpermeabilized cells expressing HA-syn1 (N-terminal HA fusion) and a syn1-HA (C-terminal HA fusion). **d** Co-immunostaining of cells expressing pkd2 and syn1-HA constructs in unpermeabilized cells

mechanosensitive ion channels (Markin and Martinac 1991; Markin and Sachs 2004). Our results at the first level indicate that plasma memebrane cup-crenellation leads to enhanced pkd2 internalization without affecting the internalization of other membrane proteins (e.g., aap1). Although amphipaths are not highly specific activators of mechanosensitive ion channels, the knowledge that the pkd complex is involved in mechanosensation suggests that the pkd2 protein in *S. pombe* may be activated by mechanosensitive forces (given also the absence of a pkd1 protein in yeast cells). Although it has been reported that pkd2 in humans is a Ca^{2+}-activated nonselective ion channel (Hanaoka et al. 2000), other TRP-like channels previously described as Ca^{2+}-activated and nonselective have been found to be mechanosensitive (Zhou et al. 2003). Gadolinium is another nonselective modulator of mechanosensitive ion channels (Petrov and Martinac 2007), again adding to the idea that pkd2 may be mechanosensitive. Our explanation for the effect of amphipaths on cell growth of the pkd2-depleted strain but not the wild-type strain is that amphipaths cause a more rapid internalization of pkd2, thus depleting pkd2 further before it is able to perform its signaling function in cell growth/cell shape. It is our theory that pkd2 is a mechanosensitive ion channel; thus, the effect of gadolinium may be to "freeze" the lipids in the membrane, inhibiting the small amount of pkd2 in the membrane of pkd2-depleted cells. At these concentrations of gadolinium the wild-type strain is not significantly affected due to the greater amount of pkd2 in the membrane. However, these findings will have to be investigated further by expression of pkd2 in *Xenopus* oocytes or *Saccharomyces cerevisiae* and patch-clamp identification of the type of channel that the *pkd2* gene encodes.

Although it was previously believed that yeast do not possess synaptotagmin, it has recently been shown that they do contain such molecules (Schulz and Creutz 2004).

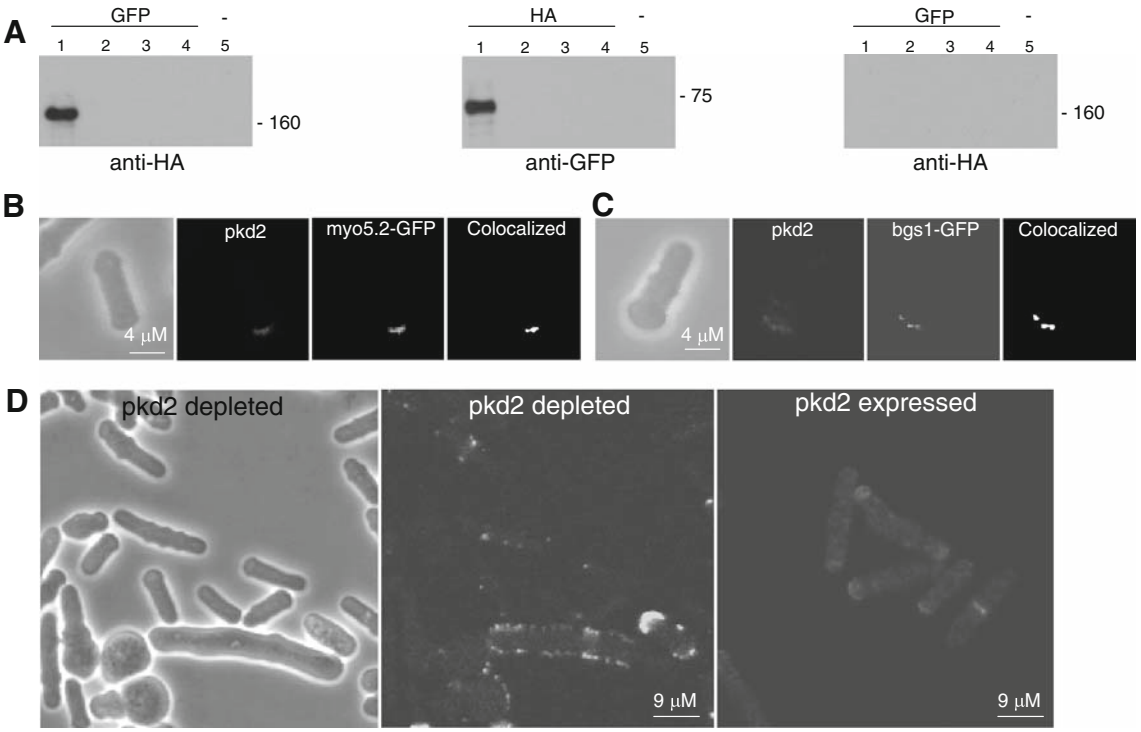

Fig. 7 Pkd2 interacts and colocalizes with myosin V and glucan synthase. **a** Western blots depicting pkd2 interaction with myo5.2 but not myo5.1. Cell lysates were prepared from cells expressing the following tagged constructs and used for immunoprecipitation. The immunoprecipitates were loaded and separated on SDS 10% PAGE and then analyzed by immunoblotting. First two panels: *lanes 1* and *5*, pkd2-myc and myo5.2-HA; *lane 2*, pkd2-myc; *lane 3*, myo5.2-HA; *lane 4*, null. Third panel: *lanes 1* and *5*, pkd2-myc and myo5.1-HA; *lane 2*, pkd2-myc; *lane 3*, myo5.1-HA; *lane 4*, null. The immunoprecipitating antibody is shown above each blot, and the antibody used as a Western blot probe is indicated below each blot. Size of marker proteins (in kDa) is indicated to the side of all blots. **b** Immunostaining of cells expressing pkd2 and myo5.2-GFP constructs in unpermeabilized cells. **c** Co-immunostaining of cells expressing pkd2 and bgs1-GFP in unpermeabilized cells. **d** Immunostaining of permeabilized cells for bgs1 following pkd2 depletion for 24 h

Studies in *Saccharomyces cerevisiae* strongly support the proposed role for these molecules in calcium-dependent membrane trafficking processes. Our results indicate that a synaptotagmin-like molecule in *S. pombe* interacts and colocalizes with pkd2. Furthermore, pkd2 was also found to interact with myosin V. Myosin V activity has been found to be necessary to efficiently localize the beta-1,3-glucan synthase bgs1, either at the cell poles or at the division septum, regions of cell wall deposition. Indeed, pkd2 depletion severely changed bgs1 localization, which is partly responsible for cell wall deposition.

Based upon our results in this study and previous investigations of pkd2 in *S. pombe* and the work of other investigators on myosin V (Mulvihill et al. 2006), bgs1 (Cortes et al. 2002) and yeast synaptotagmin homologues (Schulz and Creutz 2004), we have formulated a hypothesis concerning the role of pkd2 in cell wall synthesis and membrane trafficking. In this model pkd2 is localized to cytoplasmic vesicles with synaptotagmin. Since myo5.2 in *S. pombe* is strongly associated with vesicle movement probably along actin cables (Mulvihill et al. 2006), we propose that these vesicles containing plasma membrane proteins (since pkd2 depletion causes abnormal plasma membrane trafficking) are trafficked toward the growing tip of the cell during the G_2 phase of the cell cycle, whereupon it is presumed that they fuse with the cell membrane, thus elongating the cell. Pkd2 localization at the cell tip is transient and quickly internalized. This process is Ca^{2+}-dependent and enhanced or inhibited by modulators of mechanosensitive ion channels. Pkd2 is found at the cell tip in a complex with rho1, the activating subunit for bgs1, which is responsible for cell wall deposition. Although we do not know the activation mechanism (but we speculate it may be mechanosensitive forces) of pkd2, we hypothesize that calcium entry through pkd2 activates synaptotagmin, which in turn leads to activation of rho1 and bgs1, resulting in cell wall deposition at the newly deposited cell membrane at the cell tip. Of note is the fact that a synaptotagmin homologue in *Saccharomyces cerevisiae* appears to be involved in a wound repair mechanism (Aguilar et al. 2007). Future studies will focus on the biophysical nature of the pkd2 channel and the activating mechanism(s) of this channel in relation to its role in cellular physiology.

Acknowledgements This research was funded by a Polycystic Kidney Disease Foundation Award. pALGms1-GFP was generously supplied by Kaoru Takegawa, pREP41 constructs were generously supplied by Iain Hagan, pJK-GFP-bgs1 was generously supplied by Juan Carlos Ribas and pREP41x-GFP-*myo5.2* was generously supplied by Daniel Mulvihill.

References

Aguilar PS, Engel A, Walter P (2007) The plasma membrane proteins Prm1 and Fig1 ascertain fidelity of membrane fusion during yeast mating. Mol Biol Cell 18:547–556

Arellano M, Duran A, Perez P (1996) Rho 1 GTPase activates the (1–3) beta-d-glucan synthase and is involved in Schizosaccharomyces pombe morphogenesis. EMBO J 15:4584–4591

Bok JW, Sone T, Silverman-Gavrila LB, Lew RR, Bowring FJ, Catcheside DE, Griffiths AJ (2001) Structure and function analysis of the calcium-related gene spray in *Neurospora crassa*. Fungal Genet Biol 32:145–158

Booher RN, Alfa CE, Hyams JS, Beach DH (1989) The fission yeast cdc2/cdc13/suc1 protein kinase: regulation of catalytic activity and nuclear localization. Cell 58:485–497

Charron AJ, Nakamura S, Bacallao R, Wandinger-Ness A (2000) Compromised cytoarchitecture and polarized trafficking in autosomal dominant polycystic kidney disease cells. J Cell Biol 149:111–124

Cortes JC, Ishiguro J, Duran A, Ribas JC (2002) Localization of the (1,3)beta-d-glucan synthase catalytic subunit homologue Bgs1p/Cps1p from fission yeast suggests that it is involved in septation, polarized growth, mating, spore wall formation and spore germination. J Cell Sci 115:4081–4096

Craven RA, Griffiths DJ, Sheldrick KS, Randall RE, Hagan IM, Carr AM (1998) Vectors for the expression of tagged proteins in *Schizosaccharomyces pombe*. Gene 221:59–68

Ding DQ, Tomita Y, Yamamoto A, Chikashige Y, Haraguchi T, Hiraoka Y (2000) Large-scale screening of intracellular protein localization in living fission yeast cells by the use of a GFP-fusion genomic DNA library. Genes Cells 5:169–190

Forman JR, Qamar S, Paci E, Sandford RN, Clarke J (2005) The remarkable mechanical strength of polycystin-1 supports a direct role in mechanotransduction. J Mol Biol 349:861–871

Hanaoka K, Qian F, Boletta A, Bhunia AK, Piontek K, Tsiokas L, Sukhatme VP, Guggino WB, Germino GG (2000) Co-assembly of polycystin-1 and -2 produces unique cation-permeable currents. Nature 408:990–994

Humphrey T, Pearce A (2005) Cell cycle molecules and mechanisms of the budding and fission yeasts. Methods Mol Biol 296:3–29

Markin VS, Martinac B (1991) Mechanosensitive ion channels as reporters of bilayer expansion. A theoretical model. Biophys J 60:1120–1127

Markin VS, Sachs F (2004) Thermodynamics of mechanosensitivity. Phys Biol 1:110–124

Moreno S, Klar A, Nurse P (1991) Molecular genetic analysis of fission yeast *Schizosaccharomyces pombe*. Methods Enzymol 194:795–823

Mulvihill DP, Edwards SR, Hyams JS (2006) A critical role for the type V myosin, Myo52, in septum deposition and cell fission during cytokinesis in *Schizosaccharomyces pombe*. Cell Motil Cytoskeleton 63:149–161

Nauli SM, Alenghat FJ, Luo Y, Williams E, Vassilev P, Li X, Elia AE, Lu W, Brown EM, Quinn SJ, Ingber DE, Zhou J (2003) Polycystins 1 and 2 mediate mechanosensation in the primary cilium of kidney cells. Nat Genet 33:129–137

Ong AC, Harris PC (2005) Molecular pathogenesis of ADPKD: the polycystin complex gets complex. Kidney Int 67:1234–1247

Palmer CP, Aydar E, Djamgoz MB (2005) A microbial TRP-like polycystic-kidney-disease-related ion channel gene. Biochem J 387:211–219

Petrov E, Martinac B (2007) Modulation of channel activity and gadolinium block of MscL by static magnetic fields. Eur Biophys J 36:95–105

Qi Z, Chi S, Su X, Naruse K, Sokabe M (2005) Activation of a mechanosensitive BK channel by membrane stress created with amphipaths. Mol Membr Biol 22:519–527

Sawin KE (2002) Cell polarity: following formin function. Curr Biol 12:6–8

Schulz TA, Creutz CE (2004) The tricalbin C2 domains: lipid-binding properties of a novel, synaptotagmin-like yeast protein family. Biochemistry 43:3987–3995

Sutters M (2006) The pathogenesis of autosomal dominant polycystic kidney disease. Nephron Exp Nephrol 103:149–155

Sveiczer A, Tyson JJ, Novak B (2004) Modelling the fission yeast cell cycle. Brief Funct Genomic Proteomic 2:298–307

Tanaka N, Takegawa K (2001) Functional characterization of Gms1p/UDP-galactose transporter in *Schizosaccharomyces pombe*. Yeast 18:745–757

Torres VE, Harris PC, Pirson Y (2007) Autosomal dominant polycystic kidney disease. Lancet 369:1287–1301

Tsiokas L, Kim S, Ong EC (2007) Cell biology of polycystin-2. Cell Signal 19:444–453

Watnick TJ, Jin Y, Matunis E, Kernan MJ, Montell C (2003) A flagellar polycystin-2 homolog required for male fertility in *Drosophila*. Curr Biol 13:2179–2184

Wilson PD (2004) Polycystic kidney disease: new understanding in the pathogenesis. Int J Biochem Cell Biol 36:1868–1873

Yoon TY, Shin YK (2009) Progress in understanding the neuronal SNARE function and its regulation. Cell Mol Life Sci 66:460–469

Zhou XL, Batiza AF, Loukin SH, Palmer CP, Kung C, Saimi Y (2003) The transient receptor potential channel on the yeast vacuole is mechanosensitive. Proc Natl Acad Sci USA 100:7105–7510